Hepatic tumors diagnosis system based on fuzzy c-means using computed tomography images

Yasmeen Al-Saeed
Mansoura University
Wael Gab-Allah
Mansoura University
Mohammed Elmogy (melmogy@mans.edu.eg)
Mansoura University

Research Article

Keywords: Liver tumors, Hepatic tumors, Computer-aided diagnosis system, Computed tomography, Liver tumors segmentations, Liver tumors diagnosis, Fuzzy c-means

Posted Date: July 18th, 2022

DOI: https://doi.org/10.21203/rs.3.rs-1746728/v1

RESEARCH

Hepatic tumors diagnosis system based on fuzzy c-means using computed tomography images

Yasmeen Al-Saeed [1,2], Wael A. Gab-Allah [1] and Mohammed Elmogy [1,*]

Abstract:

Background: Liver cancer due to hepatic tumors is one of the primary mortality causes globally. Detecting and diagnosing such tumors can be very tricky in reducing death rates. Segmenting liver tumors from computed tomography (CT) images is a very tricky and challenging task due to many factors such as fuzziness of the liver intensities range, liver pixels intensities values intersection with the neighboring abdomen organs, noise imposed by CT scanner, and variance in tumors and appearances. This paper introduces a Computer-Aided Diagnosis (CAD) system based on some of the Fuzzy C-means (FCM) method variations to detect liver tumors on CT images. Furthermore, one of the main objectives of this paper is to diagnose and label detected liver tumors, either benign or malignant.

Methods: Multi-scale Fuzzy C-Means (MSFCM) is used as the liver segmentation method, and its output is the liver segmented out of the abdomen CT image. In order to achieve high-quality liver tumors segmentation, the segmentation is done using two FCM algorithms; Gaussian Kernelized Fuzzy C-Means (GKFCM) and Fast Generalized Fuzzy C-Means (FGFCM), respectively. The diagnosis is achieved by extracting features from segmented tumors and passing them to the support vector machines (SVM) classifier.

Results: To evaluate the overall performance of the proposed CAD system, the system was implemented using CT images from three liver benchmark datasets with a total of 250 subjects. The used datasets are MICCAI-Sliver07, LiTS17 and 3Dircadb. Different performance metrics were calculated, such as accuracy (ACC), sensitivity (SEN), specificity (SPE), and dice similarity score (DSC). The proposed system achieved reasonable performance results with an average ACC, SEN, SPE, and DSC of 96.62%, 95.84%,94.20%, and 95.21%, respectively.

Conclusions: The proposed system was able to differentiate benign and malignant tumors with reasonable accuracy. The resulted accuracy resulted from our CAD system features such as noise robustness, detail persevering, and being a fully-automatic system with no need for user interaction. The experimental results showed the applicability of the proposed system using different liver datasets.

Keywords: Liver tumors, Hepatic tumors, Computer-aided diagnosis system, Computed tomography, Liver tumors segmentations, Liver tumors diagnosis, Fuzzy c-means.

Background

The liver plays a vital role in the human body. It takes the responsibility of administrating and performing more than 500 essential functions.

[1],* Correspondence: melmogy@mans.edu.eg

[1]Department of Information Technology, Mansoura University, Mansoura, Egypt.

A full list of author information is available at the end of the article.

Liver functions include blood clotting regulation, blood filtering and raising the body's immunity against infections. Hence, any liver problem will affect the health of the human body. More than 40,000 adults are expected to be diagnosed with primary liver cancer in the US this year according to the American Cancer Society (ACS), The recent death rates due to liver cancer compared to those of 1980 have increased

three times [1]. Liver cancer is ranked as the 5th and the 7th death caused by cancer for men and women, respectively. It causes almost 30,000 deaths each year [2]. This makes the process of liver tumor detection one of the essential tasks in reducing morbidity or death rates.

One of the most critical research issues in the radiology field is the early detection and diagnosis along with the staging of chronic liver diseases (CLDs). Tumors mostly cause CLDs, and their development can be divided into many stages with different physiological and pathological characteristics. The early stage of liver cancer as CLD is called fatty liver infiltration or steatosis, by which fats increase in hepatocytes [3]. As cancer develops to the critical stage by which the liver enters the damage stage, liver fibrosis starts to exist. The development of fibrosis is highly dependent on the source of liver failure, such as chronic hepatitis. The evolution of cirrhosis is the very late stage of liver cancer as CLD. Cirrhosis appearance indicates long-term liver damage that affects its functionality [4]. When cirrhosis develops in late stages, the case diagnosis is primary liver cancer or hepatocellular carcinoma (HCC) [5].

The staging of CLD can be subdivided into two steps, detection and diagnosis of tumors. The staging can be achieved by using computer-aided diagnosis (CAD) systems and medical imaging modalities [6]. CAD systems consist of computer algorithms and methods to extract hidden knowledge from medical images/scans from different medical imaging modalities. The main concern of CAD systems is to enhance the quality of diagnosis and the process. Computed tomography (CT) imaging modality is the most popular imaging modality in use when designing hepatic tumors CAD.

CAD development is one of the hottest research topics in the computer-aided medical field. The main objectives of hepatic or liver CAD systems development research can be enumerated as follows; improving medical images quality using enhanced and efficient algorithms and techniques, segmentation, and detection of liver tumors while keeping a tradeoff between segmentation accuracy and implementation efficiency, labeling detected liver tumors with their medical categories and names such as labeling a detected liver tumor into benign (category) and cyst (medical name) [7]. The process of segmenting liver tumors from CT scans can be done either manually by radiologists or automatically with the aid of CAD.

Tumor manual segmentation is a tedious and excessively time-consuming process in a clinical-experimental setting. On the other hand, the process of automatically segmenting liver tumors is very challenging for several reasons. Some of these reasons appear when a tumor is segmented with the liver segmentation as an intermediate stage. The other part of the problem is related to the tumor segmentation process itself. Segmenting the liver first and then using the segmented liver area to segment out tumors will be advantageous in reducing the error rates resulting from segmenting abdomen organs as tumors.

The first problem appears with the liver segmentation from neighboring abdomen organs as the liver stretches through 100 slices with different shapes and sizes through CT slices in a CT volume. The second problem is the huge intensities of intersection between the liver and other neighboring organs. The tumor segmentation problems include indefinite tumor shapes and appearances, low-intensities contrast with huge intensities overlap between tumors and the liver areas. All those problems together make the tumor segmentation process challenging and difficult [8].

We can divide the segmentation methods used in the segmentation process into semi, interactive, or fully automatic methods. The most common segmentation techniques used to build a liver segmentation method are based on approaches such as histogram, region, edge, model, watershed, and fuzzy logic methods [9-10]. Table 1 compares some of the most popular segmentation methods in terms of their complexity, speed, advantages, disadvantages, suitability, and applicability.

The main challenges related to the liver tumors segmentation task can be enumerated as follows. When the liver is first segmented as an intermediate stage before tumor segmentation, problems related to liver segmentation appear, such as the high ambiguity between the liver and its surrounding organs, especially the heart, right kidney, and spleen. Second, the liver and tumors can have several shapes, sizes, and appearances across CT slices for the same subject and different subjects. Finally, the existence of tumors may cause severe intensity inhomogeneity [11].

After the successful segmentation of liver tumors, the tumor diagnosis stage starts by which detected tumors are labeled. CAD system diagnoses liver tumors by labeling segmented tumors by either their category (i.e. malignant or benign) or by their medical names such as cyst or HCC. The labelling process is implemented as a classification task which needs features to be extracted from tumors areas.

Tumors features are the quantitative measurements that best characterize tumors areas. Classification accuracy is directly proportional to the extracted features' quality. To reduce the complexity of the classification process and to enhance the efficiency, a features selection stage is added to CAD systems to select the most tumors characteristic features. Some search strategies such as exhaustive, heuristic and non-deterministic approaches are used to build feature selection methods [12].

Liver tumor features are mainly divided into two main categories, namely textural and statistical features. Textural-based features indicate the change in appearance and textural variance between benign and malignant tumors. Homogeneity, Gabor energy, energy, contrast, and correlation are examples of textural features. Statistical-based features indicate the changes in intensities values between benign and malignant tumor tissues and include uniformity, entropy, variance, and mean [12].

Table 1 Comparison of Popular Image Segmentation Methods.

Criteria	Fuzzy-Based	Thresholding	Region-Based	Edge- Based	Watershed-Based
Complexity	Moderate	Low	High	Low	Moderate
Noise Sensitivity	Yes	Yes	Yes	Yes	Yes
Advantages	Efficient method reasonable coverage.	Result in reasonable accuracy when used with greyscale images or for the task of image linearization. Prior image information is not required.	Provide an exact image with clear edges. Require a small number of seed points for function, probably.	Edge-based methods without any prior knowledge about image content.	Classify the pixels of images based on their intensities.
Disadvantages	The output is highly dependable on the number of partitions used for segmentation. A fuzzy member's identification process is difficult.	Threshold selection is critical and difficult.	Difficult to determine the number of optimal classes. Difficult spatial information utilization. Complex features extraction process.	Low segmentation quality if the image contains too many edges.	The usage of pixel intensities for pixel separations may lead to over-segmentation.
Suitability	Suitable to be used rather than K-Means, and it gives better results.	Used in real-time applications	-	Suitable with images with a low number of edges.	-
Applicability	Yes	Yes	No	Yes	Yes

The sophisticated liver tumors classification task, which aims to label detected tumors into their categories and medical names, needs some sophisticated features to be used along with conventional statistical and textural features [13]. Those sophisticated features include first-order statistics (FOS), spatial gray-level dependence matrix (SGLDM), gray-level difference matrix (GLDM), Laws' texture energy measures (TEM), and fractal dimension measurements (FDM).

Methods proposed to solve liver and tumor segmentation problems using CT scans fall either direct or indirect. The direct methods segment tumors directly without segmenting the liver first. Indirect methods segment the liver first as an intermediate stage for tumor segmentation.

Moltz et al. [14] proposed a hybrid indirect technique for liver tumor segmentation. They started by adaptive thresholding rough segmentation to segment the liver. Then a model-based morphological method was applied to segment tumors. The main limitation of their technique was its dependency on the user choice for the region of interest (ROI) center points. Huang et al. [15] proposed a fully automatic hybrid technique for liver tumor segmentation. Their method used some input information to detect the liver intensities. They combined atlas-based affine and non-rigid registration to achieve automatic detection of ROI. To enhance the accuracy of tumor segmentation, tumors were segmented using pixel intensities along with some prior knowledge. The experimental outcomes indicated the applicability of this method for clinical application.

Wong et al. [16] proposed a region-growing based semi-automatic method for liver tumors segmentation using CT scans. They applied knowledge-based rules were set to make the region growing process in terms of shape and size within adequate limits. This method suffered mainly from requiring user interaction to specify two main points before the region growing process manually. Li et al. [17] proposed a hybrid method based on fuzzy C-means (FCM) and level-set approaches to segment liver tumors. The actual tumor segmentation was implemented using FCM. The segmentation output was refined using the level set approach. The main limitation of this method was the high processing time imposed by the level set technique.

Zhou et al. [18] evaluated three liver segmentation methods based on semi-automatic approaches. Those methods include knowledge-based constraints region growing method, tumors pixels clustering using propagational learning method, and Bayesian-based region method. Experimental results indicated that the first two methods had higher accuracy when compared with the third method. Pohle et al. [19] proposed an automatic segmentation method based on the adaptive region growing technique. This method was able to identify ROI by automatically acquiring homogeneity characteristics automatically. If the segmented ROI was heterogeneous, this method failed to provide reasonable segmentation quality and led to under-segmentation.

Massieh et al. [20] proposed hepatic/liver tumor segmentation from CT scans based on an enhanced threshold-based method. This method started by adding each

CT scan to enhance the contrast of CT scans. Contrast enhancement was effective in improving the quality of tumor segmentation. The main limitation of this was its high sensitivity to noise, which affected the overall accuracy. Accuracy was enhanced using roundness and knowledge acquired from neighboring slices. Danciu et al. [21] proposed using textural features such as volume, diameter, and size-to-region ratio for tumor segmentation and characterization texture. This method had the advantage of selecting unique features with minimum redundancy and a maximum dependency approach.

Ji et al. [22] proposed a hybrid method based on a combination of structural and contextual features for tumor segmentation. This method was able to learn about implicit tumor characteristics automatically by using the active contour model (ACM). Segmentation refinement was achieved using the mean shift method. Experimental results indicate the applicability of this method since it showed reasonable segmentation accuracy by combining multiple atlas scans. However, this method required user interaction to manually specify ground truth (GT). Smeets et al. [23] proposed a level set-based method to segment liver tumors. Their method started with spiral scanning by assigning a seed point inside tumor areas. Then, the level set method is applied according to a speed image. The seed image was obtained using supervised learning with statistical pixel classification. This method could not automatically identify the seed points in the middle of tumors and required the user to specify them manually.

Moghe et al. [24] proposed a threshold-based automatic tumor segmentation method from CT scans. This method had two thresholds, and their values were selected using statistical and texture measures. However, choosing threshold values was a very challenging task. Nural and Hans [25] proposed a tumor segmentation method for the liver area. First, they started by segmenting the liver using a combination of morphological and graphical methods. Then, tumors were segmented by integrating anisotropic diffusion, adaptive thresholding, and connected component algorithms. Kumar et al. [26] proposed an automatic method to segment liver tumors efficiently using CT scans. Their proposed method started by segmenting the liver using the confidence connected region growing technique. Then, tumors were segmented using alternative FCM clustering. They validated the performance of their method using 10 CT volumes.

Zhao et al. [27] proposed a liver segmentation method by integrating FCM and multilayer perceptron. The applicability of their method was validated using 10 CT volumes with 40 slices per volume. Before the actual segmentation, the quality of CT volumes was enhanced. The initial liver segmentation at which the boundaries of the liver were de-lined was achieved by implementing FCM along with morphological reconstruction filter. Then, the output from the initial segmentation was used in the training stage of the multilayer perceptron neural network. The stop condition was to stop training whenever the network could differentiate the liver areas successfully. Hame [28] proposed a hybrid tumor segmentation method using morphological features and thresholding techniques. Liver segmentation refinement was achieved using the FCM method. Liver tumor segmentation was achieved using building a geometric deformable model and then fitting the generated model. The used model was built using the FCM membership function.

Adcock et al. [29] proposed a hepatic CAD system to diagnose and label tumors as cysts, metastases, and hemangiomas. Their system used 2D persistent homology, bottleneck matching, and SVM for liver segmentation, tumor segmentation, and tumor classification. Their system produced an output that many machine learning algorithms can reuse. However, the experimental results showed poor segmentation and misclassification with large tumors.

Huang et al. [30] proposed a binary tumor classification method for labeling benign or malignant tumors. Their method segmented tumor areas using the FCM clustering method. Fast Discrete Curvelet Transform (FDCT) was used to extract tumor features. The extracted features were passed to a feed-forward classifier in order to label tumors.

Li et al. [31] proposed a hybrid technique for tumor classification from CT scans. This method is considered a method with a high dependency on the radiologist. The applicability of this method was maximized when the radiologist identified the tumor region prior to the segmentation process. The usage of some sort of prior knowledge decreased the time required for segmentation and minimized the complexity of the feature extraction task. Extracted features were spatial domain features such as dependency, run length, and different metrics. Tumor classification was achieved using Multiclass SVM (MSVM) to classify liver regions into healthy liver regions, primary hepatic carcinoma affected regions, or hemangioma regions. MSVM used the normal binary SVM classifier to perform actual classification by breaking the non-binary class classification tasks into a series of binary classification tasks.

The problem of liver segmentation task automation is still an open research point. Automatic methods usually fail with enormous and complex liver shapes through CT slices. Complex liver shapes increase the needed processing time for the training stage. This makes most of the proposed liver segmentation semi-automatic methods.

Semi-automatic segmentation methods are superior when it comes to segmentation accuracy. This is because it makes the process of liver and tumor differentiation a simpler task by allowing computer capabilities and user interaction to complement each other. However, the segmentation accuracy is directly proportional to the user skills and may be affected by user errors and biases.

Despite the rapid vast advances in liver image analysis, there are some key challenges that remain unsolved. First is the noise sensitivity of segmentation methods. Segmentation methods with low noise robustness may fail to de-line liver and tumor areas accurately. Second, the automatic methods are usually time hunger methods which consume a long

processing time. The longer the processing time, the higher the implementation complexity. Finally, the liver and abdomen organs of high intensities intersection may result in false segmentation.

This paper proposes a CAD system that aims to solve those problems. The proposed system has the ability to overcome the problem related to automation level and resulting segmentation quality due to the variance of the liver shapes through CT slices. This was achieved by creating 2D CT scans from 3D CT volumes by adding each volume's CT slices to each other.

The proposed CAD system overcame the noise sensitivity problem using color mapping, contrast enhancement, and median filtering. Median filter reduces impulse noise generated by CT scanner while color mapping and contrast enhancement enhance the quality of CT scan. The resulted filtered, color-mapped, and contrast-enhanced scan improved segmentation process quality. The proposed method uses FCM methods for segmentation stages with low noise sensitivity and high detail-preserving abilities. The used FCM methods include Multi-Scale Fuzzy C-Means (MSFCM), Gaussian Kernelized Fuzzy C-Means (GKFCM), and Fast Generalized Fuzzy C-Means (FGFCM) segmentation methods. Combining the preprocessing stage with the usage of the FCM method with low noise sensitivity produced reliable segmentation results and solved the problem of segmentation-noise sensitivity.

Finally, the proposed CAD system produced low rates of false segmentation and solved the problem of the liver-neighboring organ intensities intersection by preprocessing stage after creating 2D abdomen scans. This resulted in efficient segmentation with low false rates.

The main objective of this paper is to propose a CAD that can efficiently segment and diagnose liver tumors. The proposed CAD system starts by creating 2D scans out of 3D CT volumes by adding volume slices to each other. Then, the quality of the generated 2D scans is enhanced using color mapping, contrast-enhancing, and filtering. 2D CT scans are homogeneous and more likely to produce reliable segmentations at this point. The actual liver segmentation in this CAD system is achieved by passing enhanced 2D liver CT scans to the MSFCM method. The segmented liver is used instead of the whole abdomen scan to reduce tumor segmentation task complexity. Reliable tumor segmentation is achieved by applying GKFCM and FGFCM and then taking the intersection between their outputs as the final tumor segmentation. The segmented tumors were then labeled into malignant or benign tumors using the support vector machines (SVM) classifier. SVM is considered computationally efficient and provides good accuracy for liver disease diagnosis problems [32].

The main objectives of this paper can be outlined as follows:

- Proposing a CAD system framework to efficiently segment and diagnosis liver tumors.
- Reducing the effect of noise on segmentation quality by creating 2D abdomen scans from each 3D CT volume and enhancing the quality of the generated 2D scans.
- Reducing false segmentation rates resulted from intensities of intersection between the liver and other neighboring organs. This was achieved by a preprocessing stage that precedes the segmentation stage. It consists of filtering using the Adaptive Median Filter (AMF), color mapping, and contrast-enhancing using Brightness Preserving Dynamic Fuzzy Histogram Equalization (BPDFHE) method.
- Producing reliable segmentation results using FCM methods with high noise sensitivity robustness and details-preserving capabilities. The proposed system used the MSFCM method for liver segmentation and the GKFCM and FGFCM method for tumor segmentation.
- Producing accurate tumor diagnosis by combing statistical intensity-based, shape-based and texture-based features rather than using features from a single category.
- Validating the applicability of the proposed system using different benchmark datasets with a total of 250 CT volumes with different performance metrics.

Methods

The main objective of the proposed CAD system is to assist radiologist diagnosis decisions by providing reliable differentiation of malignant and benign liver tumors. The proposed framework can be divided into four main stages, 2D CT scan creation, 2D scan quality enhancement, segmentation, feature extraction, and tumor classification. Fig. 1 illustrates the workflow of the proposed CAD system.

The CAD systems start by converting datasets' CT volumes into 2D scans. The generated 2D scans are then color mapped into greyscale, contrast-enhanced using BPDFHE, and noise reduced using AMF. The 2D CT scans are homogeneous and more appropriate for segmentation at this point. The actual liver segmentation is achieved using the MSFCM method. Then, tumors are segmented using a segmented liver area rather than a full abdomen scan. Tumor segmentation is achieved by applying GKFCM and FGFCM methods and then taking the intersection between their outputs as the final tumor segmentation. After the successful segmentation of liver tumors, the classification or diagnosis stage starts by extracting some shape, textural and statistical features from tumor areas. Extracted features determine the quality of the tumor labeling stage. The labeling, diagnosis, or classification of tumors is achieved by passing segmented tumors along with the extracted features to SVM. The proposed CAD system could reliably label segmented tumors into malignant or benign tumors.

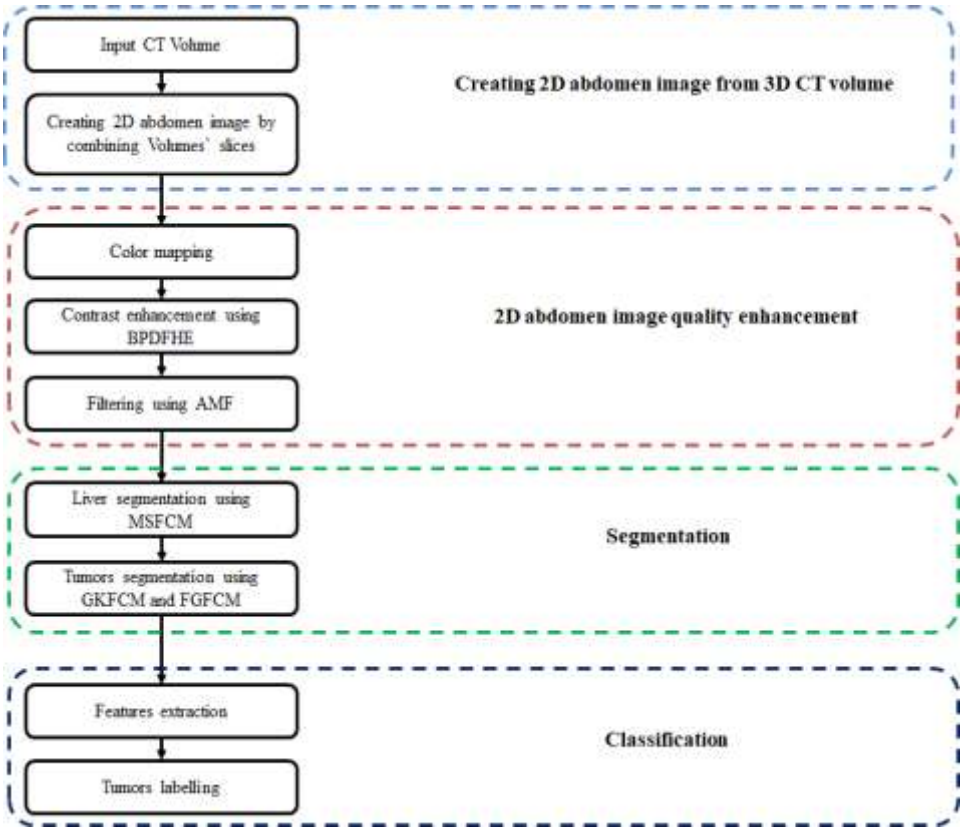

Figure 1 The proposed CAD system framework for the segmentation and diagnosis of liver tumors can be divided into four main stages, 2D CT scan creation, 2D scan quality enhancement, segmentation, features extraction, and tumor classification. The input CT scans are CT volumes from benchmark datasets; MICCAI-Sliver07, 3Dircadb, and LiTS17 datasets. Each CT volume's slices are combined to create a single 2D image for each volume. The quality enhancement stage aims to improve the quality of the segmentation stage by reducing CT noises. This is mainly because segmentation methods have high noise sensitivity. The segmentation stage aims mainly to segment hepatic tumors by first segmenting the liver. Using the segmented liver to segment tumors is beneficial for reducing error rates. Since the quality of the classification stage is highly dependable on the extracted features' quality, features from different categories are extracted.

Creating 2D CT Scans

CT imaging modality produces slices or cross-sectional images of the imaged organs, such as the abdomen organs. The CT scanner uses rotating X-ray beams around the abdomen section of the body to acquire abdomen slices. After the completion of the acquisition process, the abdomen slices and 3D CT volumes are created. CT is the most preferred imaging modality for organs tissues imaging, such as the liver. CT scanner can acquire an image of body organs in a relatively short time (i.e., 0.4 seconds). This paper uses CT volumes from benchmark datasets which are the Computer-Assisted Intervention Society MICCAI- Sliver07 dataset [33], IEEE International Symposium on Biomedical Imaging LiTS17 dataset [34], and Research Institute against Digestive Cancer 3Dircadb dataset [35]. MICCAI- Sliver07 dataset is a liver segmentation dataset. The LiTS17 and 3Dircadb datasets fit tumor segmentation with liver tumors presented in 75% of the subjects in the 3Dircadb dataset. Table 2 discusses the main characteristic of the used datasets.

To create 2D abdomen scans out of 3D CT volumes, each volume slice is added to each other. This will be beneficial in facilitating the segmentation process by reducing the complexity of computation processing.

Table 2 Characteristics of MICCAI-Sliver07, LiTS17, and 3Dircadb datasets.

Dataset	Format	No. of Subjects	No. of Slices per Subject	No. of Pixels
MICCAI-Sliver07	RAW	30	64 to 502 slices	512× 512
LiTS17	RAW	200	42 to 1024 slices	Vary through subjects
3Dircadb	DICOM	20	74 to 260 slices	512× 512

Produced 2D Image Quality Enhancement

The main purpose of this stage is to enhance the quality of the produced 2D abdomen scans to improve the quality of the segmentation process and reduce false segmentation rates. This is because the ROI is relatively more differentiable in the enhanced image. The task of liver segmentation out of the rest of the abdomen organs may point out the significance of this stage. The liver intensities values have a high intersection with other abdomen organs, which results in under or over-segmentation when applying segmentation methods. This stage also was beneficial in reducing the effect of noise sensitivity on segmentation quality.

Quality enhancement tasks can be subdivided into three main tasks; color mapping, contrast enhancement, and noise reduction. Color mapping reduces input images' color range complexity by mapping the original color range of the input images into a new range with fewer colors. For the proposed CAD system, datasets with RAW CT scans (i.e., MICCAI-Sliver07 and LiTS17 datasets) were color mapped to the range of 0 and 255, while those scans with DICOM format (i.e., 3Dircadb dataset) were color mapped to the range of −1000 to 4000 on Hounsfield scale [36]. The color-mapped abdomen scans are then contrast-enhanced using BPDFHE [37]. BPDFHE can reduce the computational processing complexity required for contrast enhancement tasks. It also has the advantage of preserving the brightness of the image. Contrast enhancement is expected to ease liver and tumor segmentation tasks by maximizing the differentiation between different image regions such as the liver and the rest of the abdomen organs, along with tumors and the rest of the liver region.

The global histogram equalization (GHE) may result in undesired artifacts and changes in image brightness. This is mainly because it remaps the local maxima of the input image histogram. The BPDFHE method only redistributes the grey level values without any histogram remapping. The BPDFHE method exploits input images' fuzzy statistics to represent and process those images. Using the fuzzy domain is advantageous in handling the large variance of grey-level values through input images. This will result in reasonable performance accuracy with low execution time. BPDFHE algorithm work as follows:

1) Computing fuzzy histogram: The fuzzy histogram denoted by *h(i)* computation starts by computing the fuzzy membership function $\mu_{\tilde{I}(x,y)i}$ as follows:

$$\mu_{\tilde{I}(x,y)} = max\left[0{,}1 - \frac{|I(x,y) - i|}{4}\right] \quad (1)$$

the fuzzy histogram is computed as follows:

$$h(i) \leftarrow h(i) + \sum_x \sum_y \mu_{\tilde{I}(x,y)i} \quad (2)$$

where $I(x,y)$ represents the original intensities values of input images and $\tilde{I}(x,y)$ represents their fuzzy representations.

2) Histogram partitioning: The fuzzy histogram is partitioned into sub-histograms using local maxima points. The actual dynamic histogram equalization is then applied upon those partitions to achieve higher contrast. The portioning process starts by identifying the local maxima using the 1st and the 2nd fuzzy histogram derivatives as follows:

$$h(i) = \frac{dh(i)}{di} \triangleq \frac{h(i+1) - h(i-1)}{2} \quad (3)$$

$$h(i) = \frac{d^2h(i)}{di^2} \triangleq h(i+1) - 2h(i) + h(i-1) \quad (4)$$

where zero-crossings correspond to the local maxima points in the 1st derivative and the negative values represent them in the 2nd derivative.

3) Span sub-histogram values: Let m_0, m_1, ……, m_n denote the local maxima detected for n+1 grey-levels. The equalization of sub-histograms may result in low-quality enhancement. This is mainly because of their small ranges. Let the original histogram be [I_{min}, I_{max}], and sub-histograms are generated to be in the ranges of [I_{min}, m_0], [m_{0+1}, m1],……., [m_{n+1}, I_{max}]. BPDHE spans sub-histograms using the total number of grey-levels in each histogram to solve the problem of sub-histograms having small ranges.

4) Dynamic histogram equalization for each sub-histogram: Each sub-histogram is mapped into a dynamic range $[\text{start}_i, \text{stop}_i]$ as follows:

$$\text{start}_i = \sum_{k=1}^{i-1} \frac{(L-1) \times [(high_k - low_k) \times log_{10} M_k]}{\sum_{k=1}^{n+1} [(high_k - low_k) \times log_{10} M_k]} + 1 \quad (5)$$

$$\text{stop}_i = \sum_{k=1}^{i-1} \frac{(L-1) \times [(high_k - low_k) \times log_{10} M_k]}{\sum_{k=1}^{n+1} [(high_k - low_k) \times log_{10} M_k]} \quad (6)$$

where $high_k$ and $low_k$is the highest and the lowest intensity values of sub-histogram k, M_k is the count of pixels with sub-histogram k, and L is the count of grey-levels. Each sub-histogram is equalized similarly to the GHE according to the total number of intensities values within each partition.

5) Image brightness normalization: The process of dynamic equalization results in brightness variance between the sub-histogram portions and the input image. To deal with such a problem, the normalization stage is required. Normalization is obtained using the following equation:

$$g(x,y) = \frac{m_i}{m_o} f(x,y) \quad (7)$$

where $g(x,y)$ represents the output contrast-enhanced image, m_i represents the mean of the

brightness of the dynamic histogram equalized image $f(x,y)$, and m_o is the mean brightness of the original input image.

The contrast-enhanced CT images are then passed to AMF to remove impulse noise imposed by the CT scanner [38]. AMF uses the adaptive window to detect the noisy pixels by comparing intensities values within the used window range. Pixels that are not structurally aligned with their neighboring pixels with large intensities variance are replaced with the median of their neighbor intensities. The AMF algorithm has the advantage of being able to maintain edges and preserves details information about the image. Using AMF and BPDFHE is very beneficial in enhancing the quality of segmentation and classification stages.

The Liver and Tumors Segmentations

The segmentation task can be subdivided into two stages; segmenting the liver out of abdomen organs and tumors segmentation out of the liver region. The proposed CAD system uses modified FCM methods named MSFCM, GKFCM, and FGFCM. The liver is segmented using the MSFCM method, while tumors are segmented using the intersection of two FCM methods; GKFCM and FGFCM.

FCM [39] is a generalization of the standard crisp C-means scheme in which all input data points are allowed to belong to all classes but with different degrees of membership. The FCM method works as follows. First, it generates C fuzzy classes or partitions and assigns *n* input points to them. Then, it assigns a center to each class. Those centers are considered clustering centers and are used by the FCM algorithm to maximize the similarity index between data points within the same class. Finally, each input point is assigned a value in the range of [0,1] to specify its degree of membership in different fuzzy classes. FCM has two main limitations. First, it eliminates the spatial dependency between input and process images as separate pixels. Second, the accuracy of its membership function is highly dependent on the similarity between pixel intensities and clustering centers. Let X indicates n input points X= X_0, $X_{1....}$, X_n, and V represents c centroids V= V_0, $V_{1.....}$, V_c, the FCM method minimalizes the Euclidean distance between X points and V centroids to classify data points into C cluster by using Eq. (8).

$$J = \sum_{j=1}^{n}\sum_{i=1}^{c}(u_{i,j})^{m} \ \| x_j - v_i \|^2 \qquad (8)$$

where $1 \leq m \leq \infty$ is the fuzzifier, v_i is the centroid corresponding to cluster C_i and $u_{i,j}$ is the membership of the pattern x_j to cluster C_i. To further reduce the implementation complexity of FCM, FCM-S1 and FCM-S2 were introduced. FCM_S1 and FCM_S2 replaced the Euclidean distance with Gaussian kernel-induced distance as follows:

$$J = \sum_{j=1}^{n}\sum_{i=1}^{c}(u_{i,j})^{m} * 1 - K(x_j, v_i) \qquad (9)$$

$$K(x_j, v_i) = \exp(-\|x_j - v_i\|^2/\sigma^2) \qquad (10)$$

When there is no-prior knowledge about noise, the original FCM and its two versions, FCM-S1 and FCM-S2 [40], have high noise and outliers sensitivity. To achieve a tradeoff between sensitivity to noise and detail preserving, a new parameter α was introduced to equation (10) as follows:

$$K(x_j, v_i) = \exp(-\|x_j - v_i\|^{\alpha}/\sigma^2) \qquad (11)$$

Selecting the optimal value of α is considered a complicated and time-consuming task. The computation complexity for segmentation using FCM-S1 and FCM-S2 is directly proportional to input image size (i.e., the larger the image, the higher the computations needed for segmentation).

When the original FCM version is used to segment noisy and in-homogenous ROI (i.e., segmenting the liver from abdomen CT scans), it may result in improper low-quality segmentation. MSFCM, GKFCM, and FGFCM methods were proposed to solve FCM problems in terms of noise sensitivity [41-43].

MSFCM method is used to segment the liver. The method starts by generating multiple scales (i.e., resolution) versions of the abdomen CT image. Then, it implements coarsest-fine clustering by which the clustering result of the coarser level $n+1$ is used for clustering's initialization at a higher scale level n. During the clustering at level $n+1$, the pixels with high membership values above a pre-defined threshold are identified and assigned to the corresponding cluster. These pixels are used to initialize the clustering at level n. The liver segmentation output results from clustering at the scale level 0. The objective function of the MSFCM at level n is given by:

$$\begin{aligned} J = &\sum_{j=1}^{n}\sum_{i=1}^{c}(u_{i,j})^{m} \ \| x_j - v_i \|^2 \\ &+\frac{\alpha}{n}\sum_{i=1}^{c}\sum_{j=1}^{n}(u_{i,j})^{m}\left(\sum_{y_r \in N_j}\|y_r - v_i\|^2\right) \\ &+\beta\sum_{i=1}^{c}\sum_{j=1}^{n}\left((u_{i,j}) - (u_{i,j})'\right)^{m}\|x_j - v_i\|^2 \end{aligned} \qquad (12)$$

where α and β are scaling factors, $(u_{i,j})'$ is the previous level's membership value resulting from clustering and is determined as follows:

$$(u_{i,j})' = \begin{cases} (u_{i,j})', & \text{if m } (u_{i,j})' > th \\ 0, & \text{otherwise} \end{cases} \qquad (13)$$

where th is the clustering threshold used to indicate pixels with the highest membership values, the value of th is usually set to 0.85.

MSFCM method enhance the quality of the liver segmentation process in terms of computational complexity and noise robustness. This is mainly because it segments ROI (i.e., the liver) using coarse to refined multi-scale clustering. The convergence of the clustering is much enhanced when

the coarser image clusters centroids are used for the next scale clustering. This is mainly because when a pixel is assigned to one cluster with a high membership value, it is expected to belong to the same cluster in the next scale and the finer image. The threshold th is used to limit the clustering in the next
scale by selecting pixels with the highest membership value. The selection of th is highly dependable on the noise level, and reliability required. A small th value is expected to be used with an image of high quality, which means more reliability when clustering the coarser image.

The proposed CAD system tumor segmentation method is considered an indirect method. This is because it requires the liver to be first segmented from the abdomen organs. Then, the segmented liver is passed to another segmentation method in order to segment existing tumors within the liver area. Segmenting tumor areas out of the liver region is advantageous in reducing false rates imposed by other abdomen organs segmented as tumors. The proposed CAD system uses GKFCM and FGFCM methods to segment tumors from the liver region. The tumors are first segmented using GKFCM and then using FGFCM. The intersection between GKFCM and FGFCM segmented tumor intensities values are used as the final segmentation result. Combing GKFCM and FGFCM improved the quality of tumor segmentation. This is mainly because GKFCM and FGFCM have high noise and outlier robustness. The preprocessing stage and using FCM that has noise robustness will be advantageous in solving the problem of low-quality segmentation resulting from high noise sensitivity.

GKFCM is the first stage in tumors segmentation and is built on the top of FCM- S1 and FCM- S2 by modifying the objective function in Eq. (9) to make it independent from the parameter α as follows:

$$J = \sum_{i=1}^{c}\sum_{j=1}^{n} (u_{i,j})^m * 1 - K(x_j, v_i) + \sum_{i=1}^{c}\sum_{j=1}^{n} \eta_i (u_{i,j})^m * \left(1 - K(\bar{x}_j, v_i)\right) \quad (14)$$

where $K(x_j, v_i)$ indicated the Gaussian kernel used, and its value is given by Eq. (10), the values of $\bar{x}$, η_i are as follows:

$$\bar{x} = \sum_{j=1}^{N} (x_k/N) \quad (15)$$

$$\eta_i = \min_{i' \neq i}\left(1 - K(v_i', v_i)\right) / \max_j \left(1 - K(v_j, \bar{x})\right) \quad (16)$$

GKFCM has the advantage of being able to learn about clustering centroid automatically using a prototype-driven learning scheme. The membership function $(u_{i,j})$ and cluster prototype (i.e., centroid) v_i are updated as follows:

$$(u_{i,j}) = \frac{\sum_{i=1}^{n} \left(\left(1 - K(x_j, v_i)\right) + \eta_i \left(1 - K(\bar{x}, v_i)\right)\right)^{-1/(m-1)}}{\sum_{j=1}^{c} \left(\left(1 - K(x_j, v_j)\right) + \eta_i \left(1 - K(\bar{x}, v_j)\right)\right)^{-1/(m-1)}} \quad (17)$$

$$v_i = \frac{\sum_{i=1}^{n} (u_{i,j})^m (K(x_i, v_i) x_k + \eta_i K(\bar{x}_i, v_i) \tilde{x}_i)}{\sum_{i=1}^{n} (u_{i,j})^m \left(K(x_i, v_i) + \eta_i K(\bar{x}_i, v_i)\right)} \quad (18)$$

FGFCM was first proposed as a solution to fix some FCM problems. It can consider the local spatial correlation between pixels during segmentation. This was achieved by changing FCM parameter α with parameter S_{kj}. This parameter integrates two parameters $S_{s,kj}$ and $S_{g,kj,}$ which denote local spatial and grey level correlation, respectively, and are defined as follows:

$$s_{kj} = \begin{cases} s_{s,kj} \times s_{g,kj}, & j \neq k \\ 0, & j = k \end{cases} \quad (19)$$

$$S_{s,kj} = exp\left(\frac{-\max(|p_j - p_k|, |q_j - q_k|)}{\lambda_s}\right) \quad (20)$$

$$S_{g,k_j} = exp\left(-\frac{\|x_k - x_j\|^2}{\lambda_g \sigma_{g,k}^2}\right) \quad (21)$$

FGFCM uses a window with the size of m*m, where x_k represents the intensity value of the window's center pixel, x_j is the j[th] pixel intensity value within the same window and λ_g represents the global spread scale factor of S_{g,k_j} . The parameter $\sigma_{g,k}$ indicates pixels' homogeneity within the local window. Small $\sigma_{g,k}$ value indicates a homogenous local window. FGFCM objective function is defined by the following equation:

$$J = \sum_{i=1}^{C} \sum_{k=1}^{q} \gamma\, \mu_{ik}^{p} (\xi_k - v_i)^2 \quad (22)$$

where v_i represents the membership degree for pixel k to class i, γ_k is the count of pixels with the same intensity as pixel k, and q indicates the count of grey levels in the input image. By incorporating spatial and grey-level correlation into the objective function, FGFCM could preserve image details with a high degree of noise robustness. FGFCM method has the advantage of being less complex and faster segmentation when compared to FCM due to its dependency on the count of grey levels rather than the total size of the input image.

Fig. 2 illustrates the experimental results of the proposed system stages. As illustrated in Fig. 2, the proposed CAD system was able to segment tumors in the case of single tumors and multiple tumors.

Features Extractions

Feature extraction is considered the most important stage for any classification task. The quality of extracted features determines the reliability and accuracy of the classification process. The proposed system implements the feature extraction stage as an intermediate stage between tumor segmentation and classification. Extracted features can be classified into three main categories which are intensity-based, texture-based, or shape-based features [44].

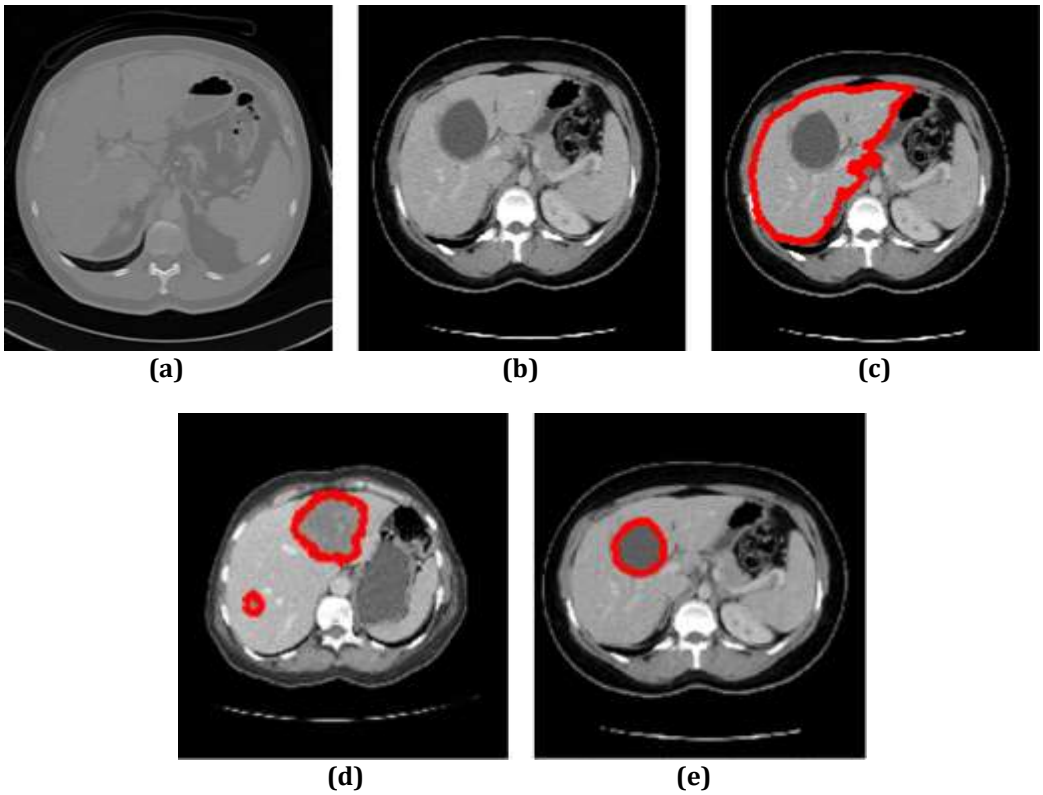

Figure 2 The proposed CAD system experimental results; (a) the produced 2D abdomen CT scan before color mapping, (b) color-mapped quality enhanced image, (c) liver segmentation using MSFCM, (d) multiple tumors segmentation using GKFCM and FGFCM, (e) single tumor segmentation using GKFCM and FGFCM.

Intensity-based tumor features are the statistical features of pixel intensities within tumor areas such as mean, variance, entropy, kurtosis, skewness, histogram, and energy of tumor areas. Textural-based features indicate the texture of the tumor areas and their homogeneities, such as Gabor-Energy and Gray-Level Difference Matrix (GLDM). GLDM matrix feature indicates different homogeneity metrics such as homogeneity-level, contrast, energy, and pixel correlation within tumor areas. Shape-based features mainly characterize different tumor shapes and include tumor area, smoothness, solidity, compactness, and sphericity.

Detected hepatic tumors can be classified using a single category of features or features from different categories to achieve more sophisticated classification, such as classifying a tumor into benign tumors first and then labeling it using its medical term, such as cyst tumor. Sophisticated classification is dependable on tumor growth patterns, patient history, and pathological features such as the presence of calcifications, fat, blood pressure, and cystic or fibrotic components [45]. The proposed CAD system uses intensity-based, shape-based, and texture-based features to cluster tumors into benign or malignant tumors. The intensity-based features are mean, variance, and skewness, GLDM as textural features, and sphericity as shape features. The mean (μ) of a tumor area indicates the statistical average of all pixels' intensities within the tumor area and is calculated as follows:

$$\mu = \frac{1}{N}\sum_{(i,j)} L_{(i,j)} \tag{23}$$

where N represents the count of tumor area pixels and $L_{(i,j)}$ is the intensity value of the tumor's pixel (i,j). The variance (σ) indicates intensities dispersion as follows:

$$\sigma = \sqrt{\sum_{h=0}^{L=1} \left(h - \bar{h}\right)^2 \cdot P(h)} \tag{24}$$

where h is the tumor area intensities histogram. A histogram indicates the count of pixels with the same intensity value (i.e., grey level) within ROI. The number of grey levels within the tumor area is in the range of [0,255]. This is mainly because the input CT scans were color mapped into a grey-level image. Skewness is related to the variance as it indicates the symmetry of the image histogram and is defined by Eq. (25).

$$\gamma_1 = \frac{1}{\sigma^3}\sum_{h=0}^{L-1} \left(h - \bar{h}\right)^3 \cdot P(h) \tag{25}$$

GLDM [45] define the existence of two intensities values regarding displacement victor δ. GLDM starts by calculating tumor area probability density function (PDF) with respect to $\delta = (\Delta x, \Delta y)$ as following:

$$D(i,\delta) = Prob[s_\delta(x,y) = i] \quad (26)$$

$$s_\delta(x,y) = |s(x,y) - s(x+\Delta x, y+\Delta y)| \quad (27)$$

where $D(i,\delta)$ is the PDF of the tumor area. The calculated PDF is further used to calculate five homogeneity-related textural features such as entropy, contrast, energy, homogeneity, and correlation as follows:

$$\text{Contrast} = \sum_x \sum_y (x-y)^2 P(x,y) \quad (28)$$

$$\text{Total Energy} = \sum_{x,y} \left(P(x,y)\right)^2 \quad (29)$$

$$\text{Entropy} = \sum_{x,y} p(x,y)\, log_P(x,y) \quad (30)$$

$$\sigma = \sum_x \sum_y (x-\mu)^2 P(x,y) \quad (31)$$

$$\text{Correlation} = \frac{\sum_x \sum_y (x-\mu_1)(y-\mu_2) P(x,y)}{\sigma_1 \sigma_2} \quad (32)$$

where $P(x,y)$ is pixels x and y GLDM-PDF. The homogeneity of the tumor area is defined by the variance. After the first and second derivatives, the mean and the variance of GLDM are represented by μ_1, μ_2, σ_1, $,\sigma_2$ respectively. Sphericity is one of the morphologic features to measure the tumor's shape. Sphericity measure is very advantageous in differentiating cysts. After completing the features extraction stage, the extracted features are used as input to SVM to label segmented tumors into either malignant or benign tumors.

Tumors Classification

Liver tumors can be defined as any abnormal growth in the liver tissues. Liver tumors are usually classified into two main categories; benign and malignant tumors. Benign liver tumors are the most common type and they are less dangerous when compared to malignant ones. Malignant tumors are the primary reason for liver cancers. Benign tumors include liver cysts, liver haemangioma and focal nodular hyperplasia. Malignant or cancerous tumors include hepatocellular carcinoma (HCC) and metastatic tumors [46]. Fig. 3 illustrates different hepatic tumors on CT scans.

Below is a brief overview of different liver tumors and their radiological characteristics.

- Cyst: Liver cysts are mainly characterized by structures containing fluids and thin walls. Tumors are ovoid or round in shape and have well-defined margins with water attenuation. Tumor quality doesn't enhance even after the contrast enhancement process.
- Liver haemangioma: Liver haemangioma is made of abnormal blood vessels and is the most common type of benign hepatic tumor. They appear in over 5% of adults around the world. They can be radiologically characterized by being iso-dense or hypo-dense to liver parenchyma.
- Focal nodular hyperplasia: Focal nodular hyperplasia tumors have the appearance of a scar and often appear in females more than males. They can be radiologically characterized by being the homogenous density of iso-dense or hypo-dense masses with a central scar.
- Metastatic tumors: Metastatic tumors appear when tumors of other parts of the body spread and reach the liver. The majority of these kinds of tumors are hypo-dense. However, they can have variable densities regarding their size and vascularity.
- HCC: HCC is the most common cancerous tumor and it mainly developed in adults with sever liver damage due to viral hepatitis. The majority of HCC tumors are iso-dense or hypo-dense.

One of the main objectives of this paper is to predict the class label for each segmented liver tumors as malignant or benign. The labelling or classification was achieved by passing the extracted features along with the segmented tumors to SVM. SVM is a binary classifier that constructs an N-dimensional hyper separation plane in order to divide the input points into two classes [47]. If the input points are not linearly separable, the current dimension must be transformed into a higher dimension. This can be accomplished using Eq. (33).

$$T_X = \phi(x) \quad (33)$$

For the classification process, a hyperplane with the largest margins separates malignant and benign classes. This is mainly because the larger the margin, the lower the classification error. SVM achieves lower processing complexity by using kernel functions such as polynomial kernel functions, radial basis function (RBF), and sigmoid and linear kernel functions [48]. Kernel functions ensure that input vectors' dot product can be computed in terms of original space variables. The proposed CAD system uses SVM with RBF as the kernel function. RBF kernel can be computed in terms of two input space's features vectors f and $\tilde{f}$ as follows:

$$RBF(f,\bar{f}) = exp\left(-\frac{\|f-\bar{f}\|^2}{2\sigma^2}\right) \quad (34)$$

where $\|f-\bar{f}\|$ denotes the Euclidian distance between f and $\tilde{f}$. As RBF is highly dependable on the distance between two vectors, the value of $RBF(f,\bar{f})$ is in the range of [0,1]. The value of 0 indicates the large difference between the two vectors, and as the value goes close to 1, then the two vectors are quite similar. RBF features space have high dimensions. Working with such dimensions is a very complex task, requiring dimension reduction. Dimensionality reduction is achieved by replacing σ in Eq. (34) with 1 as follows:

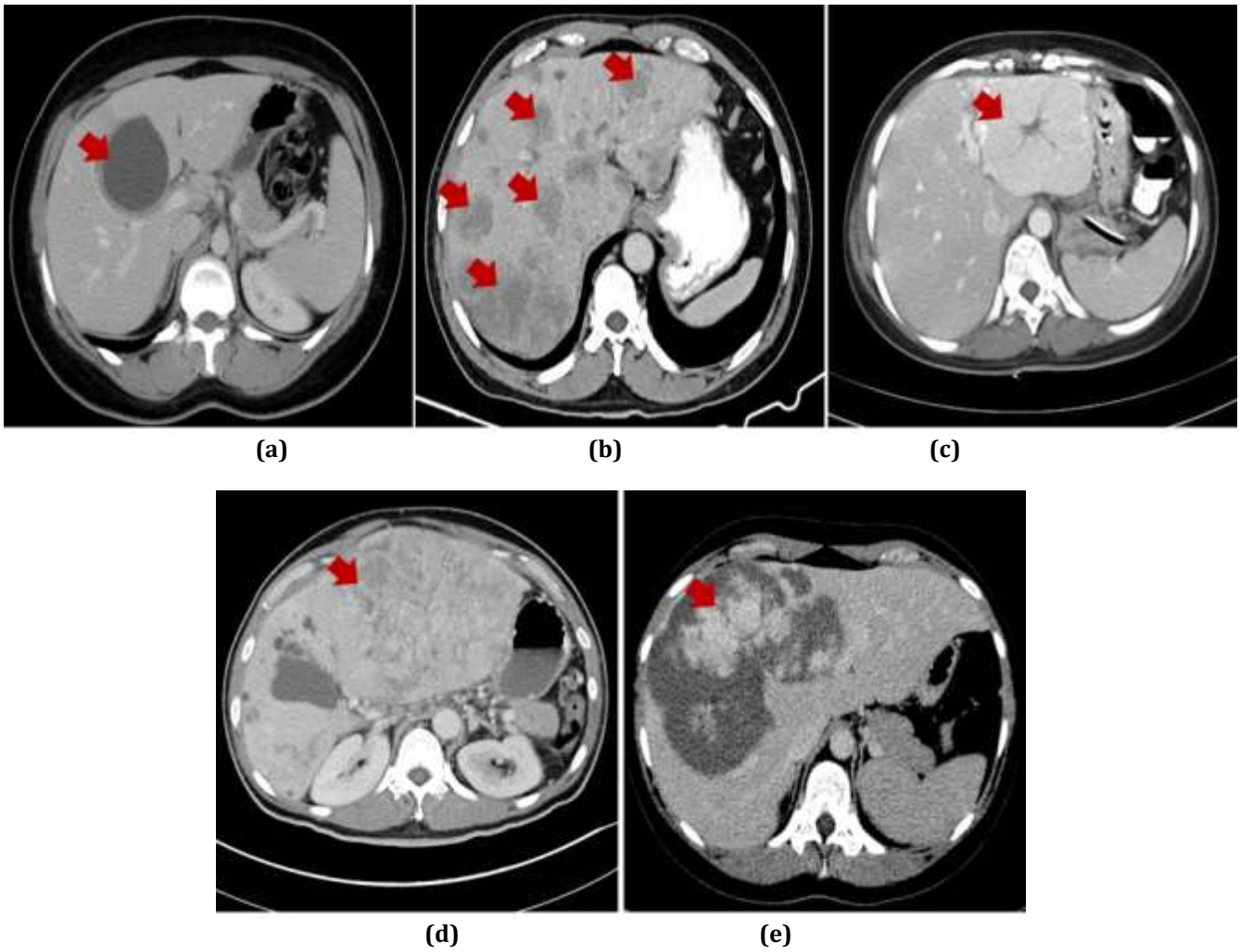

Figure 3 Hepatic tumors; (a) cyst tumors which round shape, (b) metastatic tumors, (c) focal nodular hyperplasia tumors have the appearance of a scar, (d)HCC caused by severe liver damage, and (e) haemangioma.

$$RBF(f,\bar{f}) = exp\left(-\frac{\|f-\bar{f}\|^2}{2(1)^2}\right) = exp\left(-\frac{1}{2}\|f-\bar{f}\|^2\right) = \sum_{j=0}^{\infty}\frac{(f^T f')^j}{j!} exp\left(-\frac{1}{2}\|f\|^2\right) exp\left(-\frac{1}{2}\|\bar{f}\|^2\right) \quad (35)$$

Results

The proposed CAD system was implemented using MATLAB R2017a with windows 10 under a processing environment of Intel Core I7 and 12 Gigabytes of RAM. The applicability of the proposed system was evaluated using 250 CT volumes from three publicly available benchmark datasets, MICCAI-Sliver07, LiTS17, and 3Dircadb datasets. The main characteristics of those datasets can be summarized as follows:

- MICCAI-Sliver07 is a RAW dataset that is mainly used for liver segmentation and has no tumors in the presented scans. It has 30 CT volumes with 64 to 502 slices per volume.
- 3Dircadb is a DICOM dataset of 20 CT volumes with 74 to 260 slices per volume. Tumors coexist in 75% of all volumes.
- LiTS17 is a RAW dataset with 200 CT volumes with 42 to 1026 slices per volume. This dataset has tumors presented in CT volumes.

Different metrics were calculated to evaluate the proposed CAD system's performance efficiency. The used performance measures include accuracy (ACC), sensitivity (SEN), specificity (SPE), Area under Curve (AUC), and the Dice similarity coefficient (DSC).

Segmentation ACC indicates the system's ability to precisely differentiate ROI (i.e., liver or tumors) out of abdomen CT scan. Classification ACC measures the system's

ability to identify malignant and benign tumors accurately. In other words, accuracy is a rate of the true results in a population and is defined as follows:

$$ACC = (TP+TN) / (TP+TN+FP+FN) \quad (36)$$

The terms TP, TN, FP, and FN, have different meanings when used to indicate the accuracy of segmentation and classification processes. To explain their meanings with the segmentation process well, let W be a set of input CT scan pixels. S is a set of segmented ROI pixels. G is a set of ground truth pixels, where S, G ∈ W.

- True positive (TP) is the number of correctly segmented ROI pixels and is defined as $TP = S \cap G$.
- True negative (TN) is the count of pixels rather than ROI that were accurately marked as out of interest area and is defined as $TN = S' \cap G'$.
- False positive (FP) is the count of input CT scans pixels that were incorrectly labeled as ROI and is identified by $FP = S \cap G'$.
- False negative (FN) is the count of ROI pixels that were falsely marked as out of interest pixels and defined as $FN = G \cap S'$.

For the classification process:

- TP is the count of accurately labeled malignant tumors.
- TN is the count of accurately labeled benign tumors.
- FP is the count of benign tumors that were incorrectly labeled as malignant.
- FN is the count of malignant tumors that were incorrectly labeled as benign.

SEN and SPE can be mathematically identified as follows:

$$SEN = TP/ (TP+FN) \quad (37)$$

$$SPE = TN/ (TN+ FP) \quad (38)$$

SEN is identified as a ratio of (TP) and is used as an indication for systems performance quality measurement in terms of correctly segmenting or labeling ROI areas.

SPE is the opposite of SEN and is identified as a ratio of (TN), and it indicates the system's ability to differentiate regions rather than ROI area correctly. The method can be precise without being sensitive, or it can be susceptible without being specific.

AUC measure is added to evaluate the classification stage. AUC indicates the quality of the experiment whenever the receiver operating characteristic curve (ROC) values tend to the upper left corner. ROC indicates the quality of the classifier by varying its discrimination threshold.

DSC is a similarity measure indicating the distance between segmented ROI or labeled ROI and the GT provided. DSC takes values in a range of 0 and 1. The value of 0 indicates low similarity, and the similarity increases as the value tend to 1. DSC is defined mathematically as follows:

$$DSC = 2\times TP / (2\times TP + (FP+FN)) \quad (39)$$

Liver and Tumors Segmentation Evaluation

The liver was segmented out of abdomen organs using the MSFCM method. Table 3 demonstrates the experimental results of liver segmentation MSFCM. Table 4 shows experimental results for the liver segmentation when MSFCM was replaced with the original FCM. From the results presented in Table 3 and Table 4, MSFCM achieves reliable segmentation with reasonable accuracy compared to the original FCM. This enhancement results from coarse to fine classification used by MSFCM since pixels with a high membership degree to one class (i.e., ROI or other than ROI) in a coarse-scale image will have a high probability of belonging to the same class at the fine-scale image. It also achieved fast segmentation results because the initial classes' centroids used for segmentation at the coarser scale improve the convergence of the MSFCM classification method.

Table 3 Experimental results for liver segmentation using MSFCM for MICCAI-Sliver07, LiTS17 and 3Dircadb datasets.

Dataset	ACC	SEN	SPE	DSC
MICCAI	97.08%	96.73%	95.53%	95.88%
LiTS17	96.52%	96.01%	94.39%	94.84%
3Dircadb	94.49%	93.50%	91.67%	93.02%

Table 4 Experimental results for liver segmentation using original FCM for MICCAI-Sliver07, LiTS17, and 3Dircadb datasets.

Dataset	ACC	SEN	SPE	DSC
MICCAI	87.00%	79.03%	81.73%	80.31%
LiTS17	85.26%	82.44%	80.09%	83.64%
3Dircadb	74.49%	79.00%	80.99%	79.05%

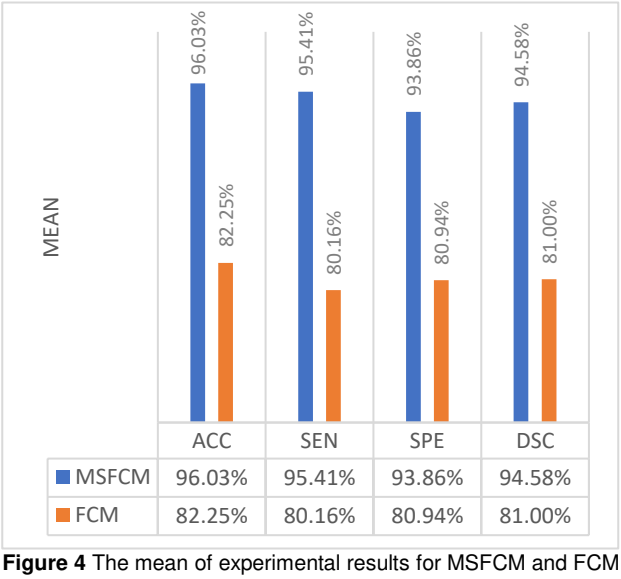

Figure 4 The mean of experimental results for MSFCM and FCM shows a huge improvement in the liver segmentation quality.

Unlike FCM, MSFCM doesn't need any user interaction to declare a tradeoff threshold between noise robustness and efficiency. This proves the reliability and automation of the liver segmentation stage using MSFCM. Figure 4 illustrates the average results for the liver segmentation using MSFCM and FCM with MICCAI-Sliver07, LiTS17, and 3Dircadb datasets. The huge improvements can be noticed regarding ACC, SEN, SPE, and DSC when MSFCM was the segmentation method in use rather than FCM.

Tumors Segmentation Evaluation

The proposed CAD system uses GKFCM along with FGFCM to segment hepatic tumors. The segmented liver area is first passed to GKFCM and then to FGFCM to produce two segmentation results. Tumors are then segmented as an intersection between the segmentation results of GKFCM and FGFCM. Tumor segmentation using GKFCM and FGFCM was evaluated using CT scans from LiTS17 and 3Dircadb datasets only. This is mainly because MICCAI-Sliver07 is a liver segmentation dataset. Table 5 presents the experimental results for the tumor segmentation stage. As illustrated by Table 5 results, the proposed tumor segmentation method resulted in reliable and reasonable outcomes.

Table 5 Experimental results for tumors segmentation using GKFCM and FGFCM for LiTS17 and 3Dircadb datasets.

Dataset	ACC	SEN	SPE	DSC
LiTS17	96.64%	95.72%	93.67%	93.82%
3Dircadb	97.00%	96.20%	94.35%	95.87%

Tumors Classification Evaluation

The performance of the tumor classification stage was evaluated with respect to the used features. Segmented tumors classification was first evaluated using SVM with statistical features only, and then it was re-evaluated when a set of statistical, textural, and shape features was--used. The used features are mean, variance, and skewness as intensity features, GLDM as texture-based features, and sphericity as shape features.The experimental results for the classification stage with only intensity-based statistical features and with statistical texture and shape features are presented in Tables 6 and 7, respectively.

Table 6 Experimental results for tumor classification using intensity-based statistical features only.

Dataset	ACC	SEN	SPE	AUC
LiTS17	76.20%	74.34%	70.99%	76.54%
3Dircadb	79.46%	75.22%	71.73%	76.31%

Table 7 Experimental results for tumor classification using SVM using intensity-based, textural and shape features.

Dataset	ACC	SEN	SPE	AUC
LiTS17	96.87%	95.53%	94.63%	96.44%
3Dircadb	97.18%	94.62%	94.85%	95.99%

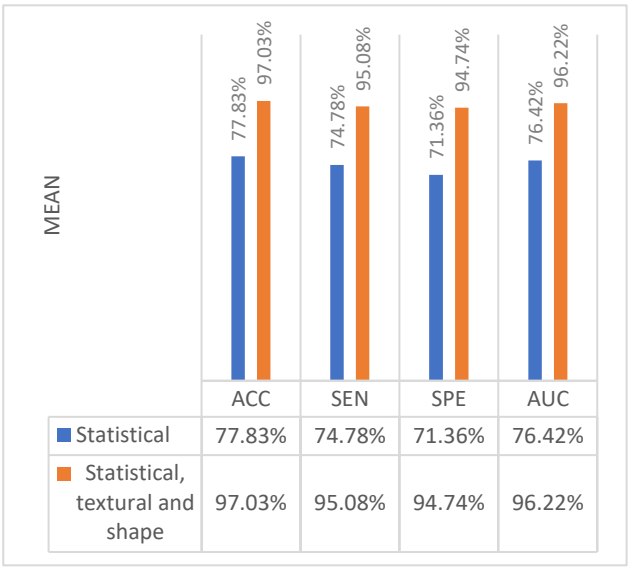

Figure 5 The mean of experimental results for the classification stage using statistical features only and statistical features along with textural and shape features.

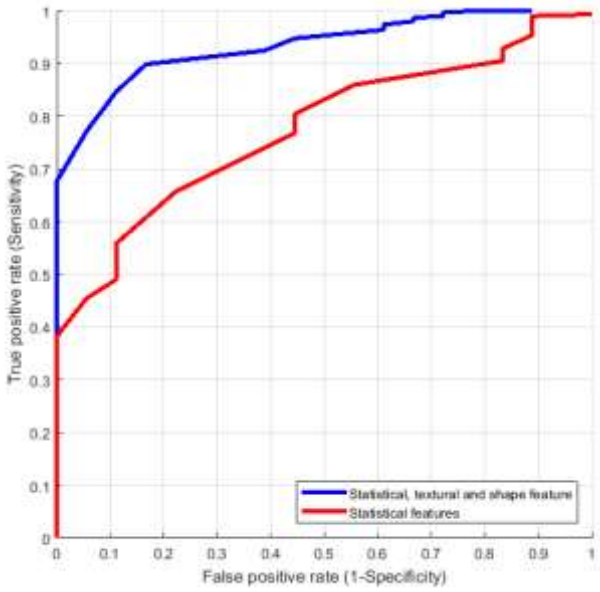

Figure 6 The ROC curves for liver tumors classification stage using statistical and combination of statistical, textural, and shape features. ROC curves indicate poor classification quality with statistical features only and reasonable quality when features from different categories are used. This is mainly because the classification with combined features tends to the upper left corner while the curve of classification with statistical features only is not.

Tables 6 and 7 illustrate that intensity-based statistical features fail to differentiate liver tumors adequately. However, when used with textural and shape features, liver tumors were well characterized and labeled as either malignant or benign. Figure 5 illustrates the mean of the experimental results for classification using intensity-based

features versus a set of intensity, textural and shape features. Fig. 6 illustrates the superiority of the proposed method in terms of tumors classification using ROC curves for different different combinations of features. As the ROC curve temds to the left upper corner, it indicates the higher quality of the system.

The Proposed CAD System Evaluation

The proposed CAD system performance evaluation as a complete system was achieved by comparing our results to other related studies which used publicly available datasets; MICCAI-Sliver07, 3Dircadb or LiTS17 datasets to evaluate their work.

For LiTS17, the proposed method reached an average ACC of 96.52%, average SEN of 96.01%, average SPE of 94.39%, and average DSC of 94.84% for the liver segmentation process. It also reached an average ACC of 96.64%, average SEN of 95.72%, average SPE of 93.67%, and average DSC of 93.82% for tumor segmentation with the same dataset. The proposed method achieved reasonable segmentation quality compared to other methods using the LiTS17 dataset, such as Pandey et al.'s [49] and Bellver et al.'s [50]. Those methods achieved an average DSC for tumor segmentation of 58.7 % and 59%, respectively. The performance evaluation results of the proposed method against other methods with the LiTS17 dataset are listed in Table 8.

Research studies implemented with the 3Dircad dataset mainly focused on the liver segmentation and less on tumor segmentation. Table 9 presents the experimental results of the proposed method against some related studies for the liver segmentation stage using 3Dircad. The proposed liver segmentation method using MSFCM and 3Dircad datasets have an average ACC of 94.49%, average SEN of 93.50%, average SPE of 91.67%, and average DSC of 93.02%. It also segment hepatic tumors using the same dataset with GKFCM and FGFCM. The tumor segmentation stage using 3Dircad reached an average ACC of 97.00%, average SEN of 96.20%, average SPE of 94.35%, and average DSC of 95.87%. From the experimental results in Tables 8 and 9, we can notice the superiority of the proposed method in tumor segmentation. The proposed CAD system performance as a complete system versus other CAD systems is illustrated in Table 10. Fig. 7 illustrates a visual representation of the DSC for the proposed method against other methods from Tables 8 and 9. Fig. 8 illustrates the superiority of the proposed method in terms of both the liver and tumor segmentation stages.

Table 8 Experimental results in terms of DSC for the proposed method using LITS17 against other methods.

Method	Liver Seg.	Tumors Seg.	Mean
Kaluva et al. [51]	92.30%	62.55%	77.40%
Bi et al. [52]	95.92%	50.00%	72.95%
Li et al. [53]	96.10%	72.21%	84.15%
Yuan [54]	96.30%	65.73%	81.00%
Our Method	94.84%	93.82%	94.33%

Table 9 Experimental results in terms of DSC for the proposed method using 3Dircad against other methods.

Method	Liver Seg.	Tumors Seg.	Mean
Chirst et al. [55]	94.3%	56.0%	75.15%
Li et al. [56]	94.5%	-	-
Moghbel et al. [57]	91.1%	-	-
Y Al-Saeed et al. [58]	92.40%	95.34%	93.87%
The proposed Method	93.02%	95.87%	94.44%

Table 10 Experimental results for the proposed CAD system against related CAD systems.

Dataset	ACC	SEN	SPE	DSC
Li et al. [53]	86.12%	87.67%	87.90%	88.85%
Doron et al. [59]	91.72%	91.00%	92.61%	90.50%
Vorontsov et al. [60]	87.62%	89.99%	85.66%	86.76%
Chlebus et al. [61]	88.13%	85.43%	87.33%	87.52%
Zhang et al. [62]	89.92%	90.25%	88.63%	89.42%
Foruzan et al. [63]	80.00%	79.61%	81.90%	82.00%
Our Method	96.62%	95.48%	94.20%	95.21%

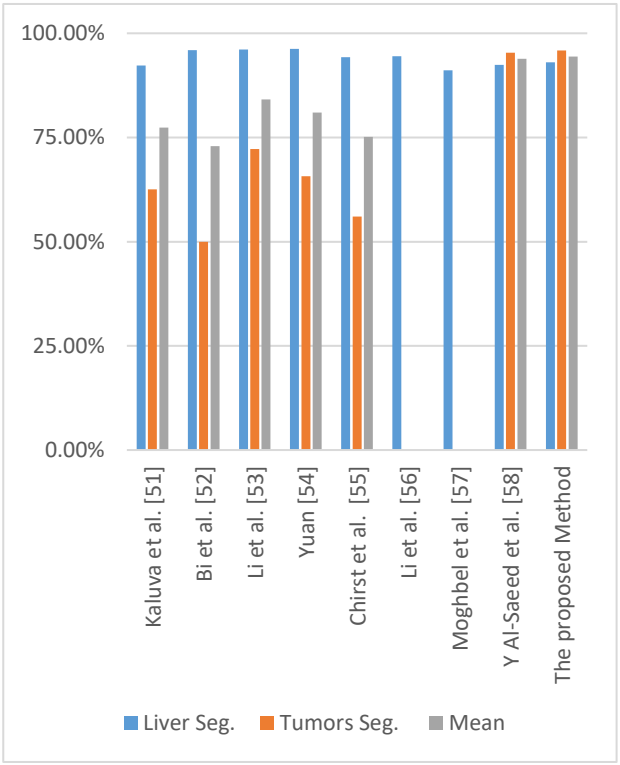

Figure 7 The proposed method DSC against other related studies. The proposed method achieved the highest average DSC in terms of liver and tumor segmentation.

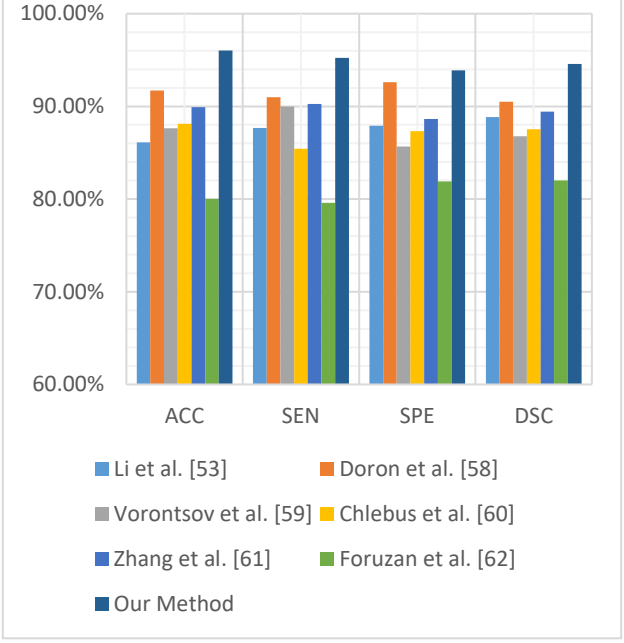

Figure 8 The proposed CAD system performance against other related CAD systems. The proposed method achieved the highest results among all presented systems in terms of ACC, SEN, SPE and DSC.

Discussion

Segmenting the liver out of the rest of the abdomen organs is an extremely tricky, challenging, and complex task. This is mainly attributable to several reasons, some are related to the nature of the liver, and some are related to the imaging modality used. The first reason is related to the liver's nature and is the huge intensities' intersection between the liver and liver-neighboring organs. This will make the process of differentiating the liver a very complicated task unless the right preprocessing is applied. The second reason is related to CT scanner noises which may result in poor segmentation quality as a result of segmentation methods' sensitivity to noise. Poor segmentation means failing to contour ROI correctly, over-segmentation or under-segmentation. The noise may also increase the processing time.

The proposed CAD system solved these problems by color mapping CT scans and enhancing their quality using AMF and BPDFHE. These pre-segmentation and quality enhancement stages were beneficial in reducing the CT noise effect. Hence, improving the segmentation quality. Besides, MSFCM is used as an actual liver segmentation method along with GKFCM and FGFCM to segment hepatic tumors. The used FCM methods have high noise robustness and detail preserving abilities while maintaining fewer complex computations. The proposed method reduced the processing complexity by combining CT slices within the same volume to produce 2D CT images for each volume.

Zhou et al. [18] segmentation method suffered from being highly dependent on the user interaction with under or over-segmentation. Luo et al. [64] used Discrete Wavelet Transform (DWT) to segment the liver. Their method achieved reasonable results with an SEN of 94.1%. However, their proposed method had high computational complexity due to DWT coefficients computations operations.

Hameed et al. [65] proposed a CAD system to differentiate malignant and benign liver tumors. Their system failed to handle high-order complex features and achieved an SEN of 84%. Chen et al. [66] proposed a CAD system to differentiate specific liver tumors called cirrhosis. This system could diagnose cirrhosis tumors only when small datasets were used and resulted in an accuracy of 90%. Edwin et al. [67] proposed a thresholding-based technique for tumor segmentation. Their method resulted in an SEN of 93%. However, selecting the optimal threshold value was very challenging and resulted in over and under-segmentation. Das et al. [68] proposed a CAD system based on adaptive thresholding. Their system resulted in an accuracy of 89.15%.

The proposed CAD system achieved an average ACC of 96.62%, an average SEN of 95.48%, an average SPE of 94.20%, and an average DSC of 95.21%. It also had the advantage of being fully automatic with high noise robustness. It also achieved low processing complexity by creating 2D CT images out of 3D CT volumes and using FCM methods with low complex operations. The proposed CAD system was able to deal with large datasets, and it achieved reliable and efficient outcomes. The proposed system applicability was verified using 250 CT volumes from three benchmark datasets.

Conclusions

This paper proposed an efficient CAD system to diagnose hepatic tumors based on FCM method variations. The proposed system was able to differentiate benign and malignant tumors with reasonable accuracy. The imaging modality used in this paper is CT. Hence, the proposed system was validated using CT volumes from three liver CT datasets; MICCAI-Sliver07, LiTS17, and 3Dircad, with a total of 250 subjects.

The proposed system started by reading 3D CT volumes and constructing a 2D CT image for each volume. This was achieved by exploiting the fact that each volume is composed of a number of slices. The proposed system constructs 2D CT images by adding each volume slice to each other. This step reduced the processing complexity that may be needed for 3D image processing. Then, the proposed system enhanced the quality of the constructed 2D abdomen CT images by making them go through the preprocessing stage. The preprocessing stage had many operations that enhanced the quality of CT scans. Those operations included color mapping, filtering, and contrast enhancement. Next, the preprocessed CT images were segmented using MSFCM into

the liver region and other abdomen regions. Afterward, the segmented liver is used to segment hepatic tumors using GKFCM and FGFCM. Using the segmented liver instead of the whole abdomen image was beneficial in reducing false rates and improving the quality of tumor detection. Finally, the segmented tumors were diagnosed as malignant or benign liver tumors by extracting some statistical, textural and shape features from tumor regions and then passing them along with the segmented tumors to SVM. Performance evaluation was achieved by calculating different performance metrics. The proposed CAD system achieved an average accuracy of 96.62%, an average sensitivity of 95.48%, an average specificity of 94.20%, and an average dice similarity score of 95.21%.

For our future work, we plan to integrate some artificial intelligence techniques into our framework. We are also planning to upgrade the classification problem to the next level by labeling segmented tumors as benign or malignant and then labeling them with their medical terms, such as HCC. This classification problem will need more efficient features that can best differentiate different liver tumors while preserving low computational time. So, the feature selection stage may be added to the next framework.

Abbreviations

CT: computed tomography, FCM: Fuzzy C-Means, MSFCM: Multi-Scale Fuzzy C-Means, GKFCM: Gaussian Kernelized Fuzzy C-Means, FGFCM: Fast Generalized Fuzzy C-Means, SVM: support vector machines, DSC: dice similarity score, ACS: American Cancer Society, CLD: chronic liver disease, HCC: hepatocellular carcinoma, FDM: fractal dimension measurements, TEM: Laws' texture energy measures, GLDM: gray-level difference matrix, SGLDM: spatial gray-level dependence matrix, FOS: first-order statistics, ROI: region of interest, GT: ground truth, ACM: active contour model, FDCT: Discrete Curvelet Transform, MSVM: Multiclass SVM, OAO: one-against-one, OAA: one-against-all, BPDFHE: Brightness Preserving Dynamic Fuzzy Histogram Equalization, AMF: Adaptive Median Filter, GHE: global histogram equalization, PDF: probability density functions, RBF: radial basis function, ROC: receiver operating characteristic curve, AUC: Area under Curve, ACC: accuracy, SEN: sensitivity, SPE: specificity, DWT: Discrete Wavelet Transform.

Acknowledgments

Not applicable.

Authors' contributions

Yasmeen Al-Saeed - Investigation, Methodology, Formal Analysis, Validation, Original Draft Preparation; Wael A. Gab-Allah- Supervision, Review and Editing; Mohammed Elmogy - Supervision, Conceptualization, Methodology, Review and Editing, Original Draft Preparation.

All authors have read and approved the manuscript.

Funding

The authors received no specific funding for this study.

Availability of data and materials

The datasets analysed during the current study are available in the ISBI challenges and the ircad institute repositories, [https://academictorrents.com/details/27772adef6f563a1ecc0ae19a528b956e6c803ce],[https://www.ircad.fr/research/data-sets/liver-segmentation-3d-ircadb-01/].

Ethics approval and consent to participate

Not applicable.

Consent for publication

Not applicable.

Competing interests

The authors declare that they have no competing interests.

Author details

1 Department of Information Technology, Faculty of Computers and Information Sciences, Mansoura University, Mansoura, 35516, Egypt. 2 Department of Information Technology, Faculty of Computers and Artificial Intelligence, South Valley University, Hurghada, 84511, Egypt.

References

1. Seco, J., Clasie, B., & Partridge, M. (2014). Review on the characteristics of radiation detectors for dosimetry and imaging. *Physics in Medicine and Biology*, *59*(20). doi: 10.1088/0031-9155/59/20/r303
2. Liver Cancer - Statistics. (2019, September 15). Retrieved from https://www.cancer.net/cancer-types/liver-cancer/statistics.
3. The Stages of Liver Disease. (2019). Retrieved from https://liverfoundation.org/for-patients/about-the-liver/the-progression-of-liver-disease/.
4. Smeets, D., Loeckx, D., Stijnen, B., Dobbelaer, B. D., Vandermeulen, D., & Suetens, P. (2010). Semi-automatic level set segmentation of liver tumors combining a spiral-scanning technique with supervised fuzzy pixel classification. Medical Image Analysis, 14(1), 13–20. doi: 10.1016/j.media.2009.09.002
5. S.gunasundari, S., & Ananthi, M. S. (2012). Comparison and Evaluation of Methods for Liver Tumor Classification from CT Datasets. International Journal of Computer Applications, 39(18), 46–51. doi: 10.5120/5083-7333
6. Li, G., Chen, X., Shi, F., Zhu, W., Tian, J., & Xiang, D. (2015). Automatic Liver Segmentation Based on Shape Constraints and Deformable Graph Cut in CT Images. IEEE Transactions on Image Processing, 24(12), 5315–5329. doi: 10.1109/tip.2015.2481326
7. Chen, E.-L., Chung, P.-C., Chen, C.-L., Tsai, H.-M., & Chang, C.-I. (1998). An automatic diagnostic system for CT liver image classification. IEEE Transactions on Biomedical Engineering, 45(6), 783–794. doi: 10.1109/10.678613
8. Hsieh, J. (2009). Computed tomography: principles, design, artifacts, and recent advances. Hoboken, NJ: Wiley Interscience.
9. Liver - Masses I - Characterisation. (2019). Retrieved from https://radiologyassistant.nl/abdomen/liver-masses-i-characterisation.
10. Blechacz, B., & Gores, G. J. (2010). Positron emission tomography scan for a hepatic mass. Hepatology (Baltimore, Md.), 52(6), 2186–2191. doi:10.1002/hep.24002

11. Ho, C.-L., Chen, S., Yeung, D. W., & Cheng, T. K. (2007). Dual-Tracer PET/CT Imaging in Evaluation of Metastatic Hepatocellular Carcinoma. Journal of Nuclear Medicine, 48(6), 902–909. doi: 10.2967/jnumed.106.036673
12. Ciurte, A., & Nedevschi, S. (2009). Texture analysis within contrast enhanced abdominal CT images. *2009 IEEE 5th International Conference on Intelligent Computer Communication and Processing*. doi:10.1109/iccp.2009.5284781
13. Kim, E. E. (2020). Artificial Intelligence and Computer-aided Diagnosis in Medicine. Current Medical Imaging Formerly Current Medical Imaging Reviews, 16(1), 1-1. doi:10.2174/1573405616012001061424 51
14. J. H. Moltz, L. Bornemann, V. Dicken and H. Peitgen (2008)."Segmentation of liver metastases in ct scans by adaptive thresholding and morphological processing", *Proc. MICCAI Workshop*, pp. 1-8, 2008.
15. Huang, C. & Jia, Fucang & Li, Y. & Zhang, X. & Luo, Huoling & Fang, C. & Fan, Y.. (2012). Fully automatic liver segmentation using probability atlas registration. International Conference on Electronics, Communications and Control 2012. 126-129.
16. Wong D, Liu J, Fengshou Y, Tian Q, Xiong W, Zhou J, Qi Y, Han T, Venkatesh S, Wang S-c (2008). A semi-automated method for liver tumor segmentation based on 2d region growing with knowledge-based constraints. In: MICCAI Workshop, vol. 41. Berlin: Springer-Verlag Berlin Heidelberg: 2008. p. 159.
17. Li, B. N., Chui, C. K., Ong, S. H., & Chang, S. (2009). Integrating FCM and Level Sets for Liver Tumor Segmentation. *IFMBE Proceedings 13th International Conference on Biomedical Engineering,* 202-205. doi:10.1007/978-3-540-92841-6_49
18. Zhou, J.-Y., Wong, D. W. K., Ding, F., Venkatesh, S. K., Tian, Q., Qi, Y.-Y., … Leow, W.-K. (2010). Liver tumour segmentation using contrast-enhanced multi-detector CT data: performance benchmarking of three semiautomated methods. *European Radiology*, *20*(7), 1738–1748. doi: 10.1007/s00330-010-1712-z
19. Pohle, R., & Toennies, K. D. (2001) "Segmentation of Medical Images Using Adaptive Region Growing," *Proceedings of SPIE Medical Imaging*, 43(22), 1337-1346. doi: 10.1117/12.431013
20. Massieh, N. H., Hadhoud, M. M., & Amin, K. M. (2010). Automatic liver tumor segmentation from CT scans with knowledge-based constraints. *2010 5th Cairo International Biomedical Engineering Conference*. doi:10.1109/cibec.2010.5716054.
21. Danciu, M., Gordan, M., Florea, C., & Vlaicu, A. (2012). 3D DCT supervised segmentation applied on liver volumes. 2012 35th International Conference on Telecommunications and Signal Processing (TSP). doi: 10.1109/tsp.2012.6256403
22. Ji, H., He, J., Yang, X., Deklerck, R., & Cornelis, J. (2013). ACM-Based Automatic Liver Segmentation From 3-D CT Images by Combining Multiple Atlases and Improved Mean-Shift Techniques. IEEE Journal of Biomedical and Health Informatics, 17(3), 690–698. doi: 10.1109/jbhi.2013.2242480
23. Smeets, D., Loeckx, D., Stijnen, B., Dobbelaer, B. D., Vandermeulen, D., & Suetens, P. (2010). Semi-automatic level set segmentation of liver tumors combining a spiral-scanning technique with supervised fuzzy pixel classification. *Medical Image Analysis, 14*(1), 13-20. doi: 10.1016/j.media.2009.09.002
24. A. Moghe, D. J. Singhai and D. S. Shrivastava (2011). "Automatic threshold-based liver lesion segmentation in abdominal 2d ct images", *International Journal of Image Processing IJIP*, vol. 5, no. 2, pp. 166-176, 2011.
25. Yussof, W. N., & Burkhardt, H. (2009). 3D Volumetric CT Liver Segmentation Using Hybrid Segmentation Techniques. *2009 International Conference of Soft Computing and Pattern Recognition*. doi:10.1109/socpar.2009.85.
26. Kumar, S. S., Moni, R. S., & Rajeesh, J. (2011). Automatic liver and lesion segmentation: a primary step in diagnosis of liver diseases. *Signal, Image and Video Processing*, *7*(1), 163–172. doi: 10.1007/s11760-011-0223-y
27. Zhao, Y., Zan, Y., Wang, X., & Li, G. (2010). Fuzzy C-means clustering-based multilayer perceptron neural network for liver CT images automatic segmentation. *2010 Chinese Control and Decision Conference*. doi:10.1109/ccdc.2010.5498558
28. Hame Y. (2008) Liver Segmentation using Implicit Surface Evaluation. The Midas Journal (2008 MICCAI workshop). 2008: 1-10
29. Adcock, A., Rubin, D., & Carlsson, G. (2014). Classification of hepatic lesions using the matching metric. Computer Vision and Image Understanding, 121, 36–42. doi: 10.1016/j.cviu.2013.10.014
30. Huang, W., Li, N., Lin, Z., Huang, G.-B., Zong, W., Zhou, J., & Duan, Y. (2013). Liver tumor detection and segmentation using kernel-based extreme learning machine. 2013 35th Annual International Conference of the IEEE Engineering in Medicine and Biology Society (EMBC). doi: 10.1109/embc.2013.6610337
31. Li, B. N., Chui, C. K., Chang, S., & Ong, S. H. (2012). A new unified level set method for semi-automatic liver tumor segmentation on contrast-enhanced CT images. Expert Systems with Applications, 39(10), 9661–9668. doi: 10.1016/j.eswa.2012.02.095
32. M. Fatima and M. Pasha, "Survey of Machine Learning Algorithms for Disease Diagnostic," Journal of Intelligent Learning Systems and Applications, vol. 09, no. 01, pp. 1–16, 2017.
33. B. Van Ginneken, T. Heimann and M. Styner, “3D segmentation in the clinic: A grand challenge,” in *MICCAI Workshop on 3D segmentation in the Clinic: A Grand Challenge*, Brisbane, Australia, pp. 7–15, 2007.
34. P. Bilic, P. F. Christ, E. Vorontsov, G. Chlebus, H. Chen *et al.,* “The liver tumor segmentation benchmark (lits)," *Computer Vision and Pattern Recognition*, vol. 1901, pp. 40–83, 2019.
35. L. Soler, A. Hostettler, V. Agnus, A. Charnoz, J. Fasquel *et al.,* "3D image reconstruction for comparison of algorithm database: A patient specific anatomical and medical image database," *IRCAD*, Strasbourg, France, Tech. Rep,, 2010.
36. Razi, T., Niknami, M., & Alavi Ghazani, F. (2014). Relationship between Hounsfield Unit in CT Scan and Gray Scale in CBCT. *Journal of dental research, dental*

clinics, dental prospects, *8*(2), 107–110. https://doi.org/10.5681/joddd.2014.019

37. Sheet, D., Garud, H., Suveer, A., Mahadevappa, M., & Chatterjee, J. (2010). Brightness preserving dynamic fuzzy histogram equalization. *IEEE Transactions on Consumer Electronics*, *56*(4), 2475–2480. https://doi.org/10.1109/tce.2010.5681130
38. Ning, C., Liu, S., & Qu, M. (2009). Research on removing noise in medical image based on median filter method. *2009 IEEE International Symposium on IT in Medicine & Education*. doi:10.1109/itime.2009.5236393
39. Bezdek, J. C., Ehrlich, R., & Full, W. (1984). FCM: The fuzzy c-means clustering algorithm. *Computers & Geosciences, 10*(2-3), 191-203. doi:10.1016/0098-3004(84)90020-7
40. Chen, S., & Zhang, D. (2004). Robust Image Segmentation Using FCM With Spatial Constraints Based on New Kernel-Induced Distance Measure. *IEEE Transactions on Systems, Man and Cybernetics, Part B (Cybernetics), 34*(4), 1907-1916. doi:10.1109/tsmcb.2004.831165
41. H. Wang and B. Fei, "A modified fuzzy c-means classification method using a multi-scale diffusion filtering scheme," Medical Image Analysis, vol. 13, no. 2, pp. 193-202, 2009
42. M.-S. Yang and H.-S. Tsai, "A Gaussian kernel-based fuzzy cmeans algorithm with a spatial bias correction," Pattern Recognition Letters, vol. 29, no. 12, pp. 1713-1725, 2008.
43. W. Cai, S. Chen and D. Zhang, "Fast and robust fuzzy c-means clustering algorithms incorporating local information for image segmentation," *Pattern Recognition*, vol. 40, no. 3, pp. 825–838, 2007.
44. Moser, T., & Nogueira, T. S. (2009). Localized Fibrous Tumor of the Liver: Imaging Features. *Liver Cancer,* 17-19. doi:10.1007/978-1-4020-9804-8_2
45. Giosa, D., Tocco, F. C., Raffa, G., Musolino, C., Lombardo, D., Saitta, C., Pollicino, T. (2020). Comprehensive characterization of HBV in tumor and non-tumor liver tissues from patients with HBV related-HCC. *Digestive and Liver Disease, 52*. doi: 10.1016/j.dld.2019.12.014
46. Characterization of Hepatocellular Carcinoma (HCC) in CT Images using Texture Analysis Technique. (2016). *International Journal of Science and Research (IJSR), 5*(1), 917-921. doi:10.21275/v5i1.nov152904
47. Terrence S. Furey, Nello Cristianini, Nigel Duffy, David W. Bednarski, Michèl Schummer, David Haussler, Support vector machine classification and validation of cancer tissue samples using microarray expression data , *Bioinformatics*, Volume 16, Issue 10, October 2000, Pages 906–914, https://doi.org/10.1093/bioinformatics/16.10.906
48. Nanda, M. A., Seminar, K. B., Nandika, D., & Maddu, A. (2018). A Comparison Study of Kernel Functions in the Support Vector Machine and Its Application for Termite Detection. *Information, 9*(1), 5. doi:10.3390/info9010005
49. Pandey, R. K., Vasan, A., & Ramakrishnan, A. G. (2018). Segmentation of liver lesions with reduced complexity deep models. *arXiv preprint arXiv:1805.09233*.
50. Bellver, M., Maninis, K. K., Pont-Tuset, J., Giró-i-Nieto, X., Torres, J., & Van Gool, L. (2017). Detection-aided liver lesion segmentation using deep learning. *arXiv preprint arXiv:1711.11069*.
51. K. C. Kaluva, M. Khened, A. Kori, and G. Krishnamurthi, "2D-Densely Connected Convolution Neural Networks for automatic Liver and Tumor Segmentation," arXiv preprint arXiv:1802.02182, 2018.
52. L. Bi, J. Kim, A. Kumar, and D. Feng, "Automatic Liver Lesion Detection using Cascaded Deep Residual Networks," *arXiv preprint arXiv:1704.02703*, 2017.
53. X. Li, H. Chen, X. Qi, Q. Dou, C. -W. Fu *et al.,* "H-DenseUNet: Hybrid densely connected UNet for liver and tumor segmentation from CT volumes," *IEEE Transactions on Medical Imaging*, vol. 37, no. 12, pp. 2663–2674, 2018.
54. Y. Yuan, "Hierarchical Convolutional-Deconvolutional Neural Networks for Automatic Liver and Tumor Segmentation," *arXiv preprint arXiv:1710.04540*, 2017
55. P. F. Christ, F. Ettlinger, F. Grun, M. E. A. Elshaer, J. Lipkova, S. Schlecht, F. Ahmaddy, S. Tatavarty, M. Bickel, P. Bilic *et al.*, "Automatic Liver and Tumor Segmentation of CT and MRI Volumes using Cascaded Fully Convolutional Neural Networks." *arXiv: Computer Vision and Pattern Recognition*, 2017.
56. C. Li, X. Wang, S. Eberl, M. Fulham, Y. Yin, J. Chen, and D. D. Feng, "A likelihood and local constraint level set model for liver tumor segmentation from CT volumes," *IEEE Transactions on Biomedical Engineering*, vol. 60, no. 10, pp. 2967–2977, 2013.
57. M. Moghbel, S. Mashohor, R. Mahmud, and M. I. B. Saripan, "Automatic liver segmentation on computed tomography using random walkers for treatment planning," EXCLI journal, vol. 15, p. 500, 2016.
58. Al-Saeed, Y., A. Gab-Allah, W., Soliman, H., F. Abulkhair, M., M. Shalash, W., & Elmogy, M. (2022). Efficient computer aided diagnosis system for hepatic tumors using computed tomography scans. *Computers, Materials & Continua*, *71*(3), 4871–4894. https://doi.org/10.32604/cmc.2022.023638
59. Y. Doron, N. Mayer-Wolf, I. Diamant and H. Greenspan, "Texture feature based liver lesion classification," *Medical Imaging 2014: Computer-Aided Diagnosis*, vol. 9035, pp. 90353K, 2014.
60. E. Vorontsov, N. Abi-Jaoudeh and S. Kadoury, "Metastatic liver tumor segmentation using texture-based omni-directional deformable surface models," in *Int. MICCAI Workshop on Computational and Clinical Challenges in Abdominal Imaging*, Cambridge, Massachusetts, USA, pp. 74–83, 2014.
61. G. Chlebus, A. Schenk, J. H. Moltz, B. V. Ginneken, H. K. Hahn *et al.,* "Automatic liver tumor segmentation in CT with fully convolutional neural networks and object-based postprocessing," *Scientific Reports*, vol. 8, no. 1, *Computer Vision and Pattern Recognition*, vol. 1901, pp. 1–7, 2018.
62. J. Zhang, Y. Xie, P. Zhang, H. Chen, Y. Xia *et al.,* "Light-weight hybrid convolutional network for liver tumor segmentation," in *Proc. of the Twenty-Eighth Int. Joint Conf. on Artificial Intelligence*, Macao, China, vol. 19, pp. 4271–4277, 2019.
63. A. H. Foruzan and Y. W. Chen, "Improved segmentation of low-contrast lesions using sigmoid edge model,"

International Journal of Computer Assisted Radiology and Surgery, vol. 11, no. 7, pp. 1267–1283, 2015.

64. S. Luo, Q. Hu, X. He, J. Li, J. S. Jin *et al.,* "Automatic liver parenchyma segmentation from abdominal CT images using support vector machines," in *2009 ICME Int. Conf. on Complex Medical Engineering*, Tempe, Arizona, USA, pp. 1–5, 2009.
65. R. Hameed and S. Kumar, "Assessment of neural network based classifiers to diagnose focal liver lesions using CT images," *Procedia Engineering*, vol. 38, pp. 4048–4056, 2012.
66. Y. W. Chen, J. Luo, C. Dong, X. Han, T. Tateyama *et al.,* "Computer-aided diagnosis and quantification of cirrhotic livers based on morphological analysis and machine learning," *Computational and Mathematical Methods in Medicine*, vol. 2013, pp. 1–8, 2013.
67. Edwin, D., & Hariharan, S. (2016). Liver and tumour segmentation from abdominal CT images using adaptive threshold method. International Journal of Biomedical Engineering and Technology, 21(2), 190. doi: 10.1504/ijbet.2016.077183
68. Das, A., Das, P., Panda, S. S., & Sabut, S. (2019). Detection of Liver Cancer Using Modified Fuzzy Clustering and Decision Tree Classifier in CT Images. Pattern Recognition and Image Analysis, 29(2), 201–211. doi: 10.1134/s1054661819020